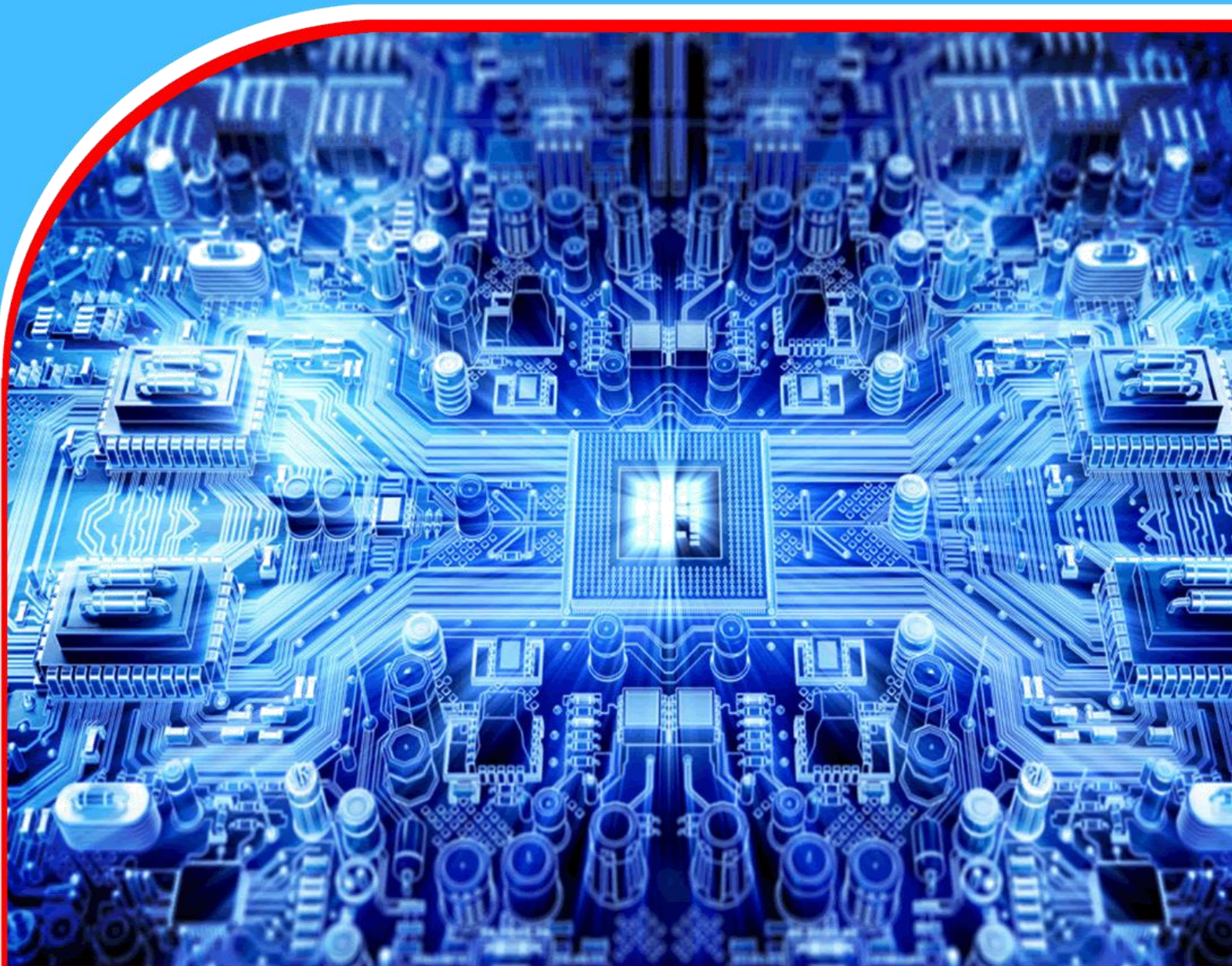


# American Journal of Computing and Engineering (AJCE)



**Application of Fractional Order PI/PID Voltage  
Controllers for Three-Phase Voltage Source Inverter  
with Dynamic Load**

*Ozan Gül*



# Application of Fractional Order PI/PID Voltage Controllers for Three-Phase Voltage Source Inverter with Dynamic Load

 Ozan Gül<sup>1</sup>

<sup>1</sup>Electrical and Electronic Engineering Department, Bingol University

 Crossref

Article history

Submitted 08.02.2024 Revised Version Received 15.02.2024 Accepted 16.02.2024

## Abstract

**Purpose:** With the depletion of fossil fuels, the landscape of electrical energy generation has witnessed a transformative shift towards alternative sources such as fuel cells and photovoltaic (PV) systems that produce direct current (DC) electricity. In the realm of distributed power generation, three-phase voltage source inverters (VSIs) are extensively utilized for converting energy from DC sources to alternating current (AC) for the grid or loads. The pivotal objective of this study is to investigate and compare the performance of fractional-order Proportional-Integral (PI) and Proportional-Integral-Derivative (PID) control structures against their integer-order counterparts in the voltage control loop of a VSI connected to a dynamic load system.

**Materials and Methods:** The research employs frequency response analysis to design and implement both fractional-order PI/PID and integer-order PI/PID control structures for the voltage control loop. The simulation of the controlled system is conducted using MATLAB/Simulink, considering two distinct test scenarios – unstable and stable dynamic load conditions. The primary focus is on analyzing the inverter output voltage in the d-q axis under these scenarios.

**Findings:** The analysis of the simulation results reveals noteworthy distinctions between the

fractional-order and integer-order PI/PID controllers in the context of controlling the inverter system with dynamic loads. These findings shed light on the advantages of employing fractional order controllers, particularly in dynamic load scenarios, showcasing superior performance in comparison to their integer-order counterparts.

**Implications to Theory, Practice and Policy:** The study's outcomes hold significant implications for the theory and practice of voltage control in distributed power generation systems. The superiority of fractional-order PI controllers underscores their potential for enhancing power quality, especially in systems with unstable and time-varying dynamic loads. These insights can inform the development of more effective control strategies for voltage source inverters, influencing both theoretical frameworks and practical applications. Policymakers may consider these findings when formulating regulations and incentives to promote the adoption of advanced control strategies in the evolving landscape of electrical energy generation.

**Keyword:** *Voltage Source Inverter, Fractional-Order PI Controller, Frequency Response Analysis, Dynamic Load, Power Quality, MATLAB/Simulink Simulation.*



## 1.0 INTRODUCTION

In the ever-evolving landscape of technological advancements, the demand for diverse forms of electrical energy continues to escalate. This surge is notably propelled by the strides made in power electronics, resulting in the development of numerous inverters catering to various applications.

Among these, three-phase voltage source DC/AC inverters stand out as pivotal power electronics converters, converting input direct voltage into different output AC voltages essential for a myriad of industrial applications requiring three-phase AC voltage. The contemporary surge in microgrid plants fueled by renewable energy sources accentuates the increasing significance of three-phase Voltage Source Inverters (VSIs) in the Power System World. Functioning with DC voltage as an input source, the VSI system contributes AC voltage or current to the load and/or grid. Achieving a clean three-phase AC waveform at the inverter output becomes imperative, posing a formidable challenge, particularly in the face of unstable and/or stable static/dynamic loads within power systems applications.

### Problem Statement

The complexity arises in controlling the output voltage to ensure high-quality energy transfer under diverse load conditions. This becomes especially challenging when dealing with dynamic loads in power systems, where the load behavior undergoes substantial variations within the same time of day, season, or even between different distribution facilities under similar weather conditions. Furthermore, the load behavior may exhibit variations between day and night under various weather conditions. Therefore, the development of control strategies for inverter systems capable of dynamically adapting to these changing load structures at each sampling time becomes imperative.

## 2.0 LITERATURE REVIEW

### Theoretical Review

Control systems have been developed to meet every need with developing technology and are used in many areas in daily life. Controllers of different structures and characteristics have been developed for industrial use and research purposes. Despite progress in control strategies, structurally simple PI, PID, and lag/lead controllers widely used in control systems. These type controllers are generally used as P, PI, PD, and PID, allows the control of systems by taking the ratio-integral-derivative values of the input and/or combinations thereof. The parameters of PID controllers can be obtained both experimentally and analytically (Åström & Hägglund, 2009; Guzmán et al, 2006). Also, the design stages do not involve further processing. Therefore, PI and

PID controllers are the most popular controllers used in the industry (Åström & Hägglund, 2009). In parallel with the developments in technology, computer-aided analysis and designs are used extensively in control systems; the use of fractional order PID ( $PI^\lambda D^\mu$ ) and PI ( $PI^\lambda$ ) controllers are becoming widespread instead of the classical PID and PI controllers. The classic PID controllers consist of three terms,  $K_p$ ,  $K_i$  and  $K_d$ , while fractional-order PID controllers have the terms  $\lambda$  and  $\mu$ , the degree of the integral operator, and the degree of the derivative operator, respectively. This allows the flexibility function to depend on five variables in the optimization process, allowing for more flexible designs. Various research in practical systems indicates that fractional-order controllers perform better related to robustness and transient response (Gül & Tan, 2019; Malek, 2014; Yang et al., 2018).

## Conceptual Framework

It is observed that the load behavior of the same distribution facilities changes greatly during the same time of day or the same season of the year, or this change may be noticed in different distribution facilities under similar weather conditions. Furthermore, the load behavior may vary between day and night in various weather conditions. Therefore, control strategies for inverter systems with dynamic load structures that changed dynamically for each sampling time must be developed.

Figure 1 shows the control structure for three-phase PWM (pulse width modulation) VSI where the voltage output voltage is controlled. A voltage control loop is used to control the VSI system to supply the desired quality AC voltage to dynamic stable/unstable loads. In this research, a fractional-order PI/PID and integer-order PI/PID controllers are designed for the voltage control loop of the inverter with the dynamic load. For this purpose, the transfer function of the considered system is obtained first. Then, the parameters of the controllers used to control the voltage control loop in the VSI system with dynamic load are designed based on the same cut-off frequency and phase margin values by utilizing the frequency response analysis of closed-loop voltage control system in this paper. For a case study, simulations are performed in Matlab/Simulink environment to compare the control performance of the integer-order controllers and fractional order controllers for the VSI system connected to stable and unstable dynamics loads conditions by using simulation results. Analyzes are made by comparing the voltage waveforms of inverter output voltages in the d-axis ( $V_d$ ) and q-axis ( $V_q$ ) and reference voltage waveforms  $V_{dref}$  and  $V_{qref}$  for the case study. The control strategy aims to regulate the voltage output from the inverter to follow a specified reference signal. So, the effect of controller structure determination on the system response is interpreted in this research. The analysis of the results shows that the superiority and the feasibility of FOPID/FO-PI controllers.

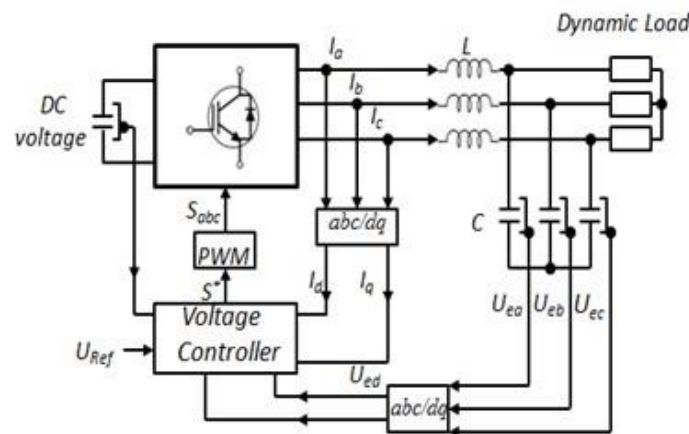


Figure 1: VSI Structure Diagram for Voltage Control

## Research Gaps

However, as technology progresses, fractional-order PID ( $PI^\lambda D^\mu$ ) and PI ( $PI^\lambda$ ) controllers are gaining prominence over classical PID controllers. The fractional-order controllers, characterized by parameters  $\lambda$  and  $\mu$ , offer more flexibility in design with five variables in the optimization process. Research indicates that fractional-order controllers exhibit superior performance in terms of robustness and transient response compared to their classical counterparts.

In the subsequent sections, this study delves into the design and analysis of fractional-order PI/PID and integer-order PI/PID controllers for the voltage control loop of a three-phase PWM (pulse width modulation) VSI, specifically addressing the challenges posed by dynamic loads in power systems. The investigation employs frequency response analysis and MATLAB/Simulink simulations to compare the control performance of both controller types under stable and unstable dynamic load conditions, shedding light on the superiority and feasibility of fractional-order controllers.

### 3.0 MATERIAL AND METHODS

#### Dynamic Load

When creating a voltage control structure for a system, load characteristics and their models should be understood. When making load models in a power system, it should be considered that there are loads with very different characteristics in the load bus bar. In a power system, electrical loads are generally analyzed in two groups: dynamic load and static load. Because static load models do not change over time and gives the current function of the bus voltage and/or frequency as the load, the traditional static loads are not enough to characterize the transient behavior of real electric loads which is driven by things such as cooking, TV, lighting, entertainment electronics, etc, so there is a necessity to design dynamic load in power system simulations to get more favorable results.

The dynamic load can be performed in the Matlab/Simulink environment by switching static load by IGBT or Breaker switches which are shown in Figure 2 (Karabiber et al., 2016). In this way, the power drawn by the static loads can be changed dynamically for each sampling time. In this study, we prefer IGBT dynamic load model because of breaker model has a snubbed capacitor which needs reactive power and ripple occur at switching time.

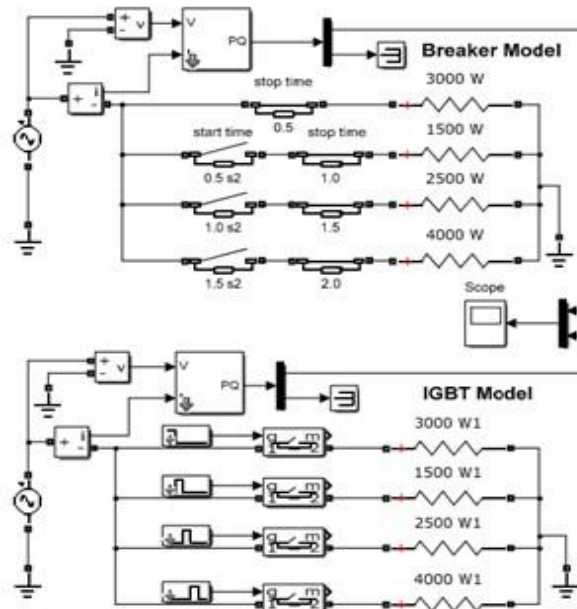


Figure 2: Dynamic Load Model Using IGBT and Breaker Switches

#### Mathematical Model of Three-Phase Voltage Source Inverter System with Dynamic Load

The circuit topology of three-phase PWM VSI is illustrated in Figure 3 (Mu et al., 2011), where  $L_1=L_2=L_3=L$ ,  $R_1=R_2=R_3=R$ ,  $C_1=C_2=C_3=C$  are inductor, resistance, and capacitor of the filter;  $u_{dc}$  is the

DC bus voltage,  $I_{DC}$  is DC side current,  $i_{Ra}$ ,  $i_{Rb}$ ,  $i_{Rc}$  are load current and  $R_L$  is the load. Moreover,  $u_{ea}$ ,  $u_{eb}$ ,  $u_{ec}$  is filter capacitance-voltage;  $i_a$ ,  $i_b$ ,  $i_c$  and  $u_a$ ,  $u_b$ ,  $u_c$  are the inverter bridge output current and voltage.

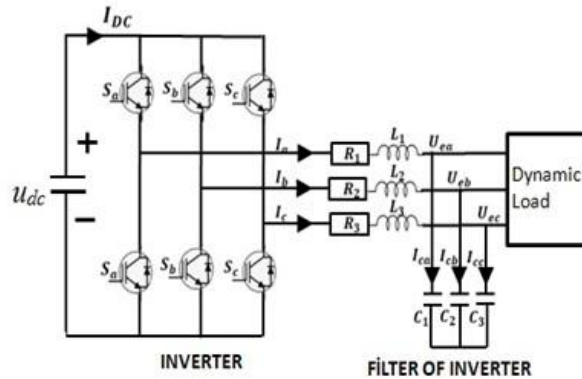


Figure 3: The Structure of Three-Phase PWM VSI

The mathematical model of the system can be obtained by using circuit equations. The voltage equations for each phase of the system are given in (1) - (4). (Malek, 2014; Mu et al., 2011).

$$L \frac{di_a}{dt} = -Ri_a + u_{dc}(S_a - \frac{1}{3} \sum_{j=a,b,c} S_j) - u_{ea} \quad (1)$$

$$L \frac{di_b}{dt} = -Ri_b + u_{dc}(S_b - \frac{1}{3} \sum_{j=a,b,c} S_j) - u_{eb} \quad (2)$$

$$L \frac{di_c}{dt} = -Ri_c + u_{dc}(S_c - \frac{1}{3} \sum_{j=a,b,c} S_j) - u_{ec} \quad (3)$$

$$C \frac{du_{ea}}{dt} = -i_{Ra} + i_a, \quad C \frac{du_{eb}}{dt} = -i_{Rb} + i_b, \quad (4)$$

$$C \frac{du_{ec}}{dt} = -i_{Rc} + i_c$$

where,  $S_a$ ,  $S_b$  and  $S_c$  are the switches in the respective phase arms.

The inverter system is a nonlinear time-varying system as can be seen in (1), (2), (3) and (4). In this research, we used Park transformation ( $dq$  transformation) to convert a three-phase, threedimensional system into a two-dimensional and also a single-phase system. If we apply  $dq$  transformation to the mathematical model of the VSI system, our new mathematical equations are;

$$L \frac{di_d}{dt} = -Ri_d + L\omega i_q + S_d u_{dc} - u_{ed} = -Ri_d + L\omega i_q + u_d - u_{ed} \quad (5)$$

$$L \frac{di_q}{dt} = -Ri_q - L\omega i_d + S_q u_{dc} - u_{eq} = -Ri_q - L\omega i_d + u_q - u_{eq} \quad (6)$$

$$C \frac{du_{ed}}{dt} = -i_{rd} + C\omega u_{eq} + i_d \quad (7)$$

$$C \frac{du_{eq}}{dt} = -i_{rq} - C\omega u_{ed} + i_q \quad (8)$$

where  $\omega$  is the angular frequency of the system and  $d$  and  $q$  represents the direct and quadrate part of parameters.

An average model of the inverter can be defined as follows (Mohan,1995);

$$u_d(t) = (u_{dc}/2) m_d(t) \quad (9)$$

$$u_q(t) = (u_{dc}/2) m_q(t) \quad (10)$$

$m_d$  and  $m_q$  are the inverter modulation signals. To decouple two nonlinear coupled terms,  $L\omega i_d$  and  $L\omega i_q$  in (5) and (6),  $m_d$  and  $m_q$  are defined as;

$$m_d = 2/u_{dc} (V_d - L\omega i_q + u_{ed}) \quad (11)$$

$$m_q = 2/u_{dc} (V_q + L\omega i_d + u_{eq}) \quad (12)$$

where  $V_d$  and  $V_q$  are two new control input signals and should be adjusted so that the inner voltage loop can be used to regulate the voltage.

(5) and (6) can be rewritten as linear time-invariant equations; by using (9), (10), (11) and (12);

$$L(di_d/dt) = -Ri_d + V_d \quad (13)$$

$$L(di_q/dt) = -Ri_q + V_q \quad (14)$$

By decoupling the current and voltage equations, the transfer function of inverter and filter will be;

$$G_{PL}(s) = V_d I_d = V_q I_q = 1/(Ls + R) \quad (15)$$

The active and reactive component of delivered power to the grid is calculated from this model as;

$$P = 3/2 (V_d i_d + V_q i_q) \quad (16)$$

$$Q = 3/2 (V_d i_q - V_q i_d) \quad (17)$$

We want the values of quadrates part of the reference voltage and current to be zero so that the reactive power drawn by the load is zero.

### Design of Voltage Controller

The purpose of this control system shown in Figure 4 (Malek, 2014) is to obtain values at the inverter output q-axis and d-axis voltages that correspond to the reference voltages we set.

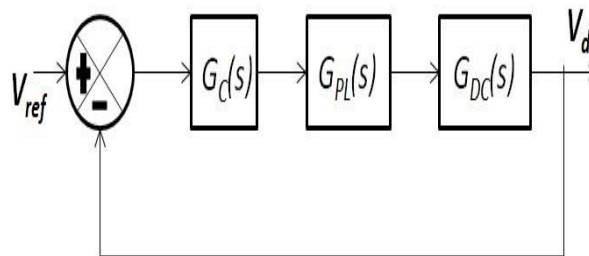


Figure 4: The Control Schematic of Voltage for the Three-Phase Inverter System

$G_c(s)$ ,  $G_{DC}(s)$  and  $G_P(s)$  are defined as respectively, the transfer function of the controller, the time delay, and noise transfer function caused by the inverter and filter of inverter and the transfer function of the inverter and filter of the inverter. The open-loop transfer function of the feedback voltage control system is founded as;

$$G_T(s) = G_{DC}(s)G_c(s)G_{PL}(s) \quad (18)$$

$$G_{PDC}(s) = G_{DC}(s)G_{PL}(s) = K_1 e^{-T_d s} / (Ls + R) \quad (19)$$

$$G_T(s) = (K_1 e^{-T_d s} / (Ls + R)) G_c(s) \quad (20)$$

### Design Specifications of Controller Turning Procedure

The transfer function of the three-phase VSI system connected to the dynamic load as shown generally in (19) is;

$$G_{PDC}(s) = K e^{-Ls} / (Ts + 1) \quad (21)$$

where  $T = L/R$ ,  $L = T_d$  and  $K = K_1/R$  are constant numbers. The transfer functions of PI, PID, FOPI and FOPID controllers that we use to control the voltage control loop at the VSI system in this study are respectively as follows;

$$PI: \quad G_{C1}(s) = K_p + K_i/s \quad (22)$$

$$PID: \quad G_{C2}(s) = K_p + K_i/s + K_d s \quad (23)$$

$$FOPI: \quad G_{C3}(s) = K_p + K_i/s^\lambda \quad (24)$$

$$FOPID: \quad G_{C4}(s) = K_p + K_i/s^\lambda + K_d s^\mu \quad (25)$$

where  $K_p, K_i, K_d, \mu \in (0, 1)$  and  $\lambda \in (0, 1)$  are considered positive real number in this research.

Several methods have been proposed to determine the parameters of PID/PI and FOPID/FOPI controllers so that the controlled system has the desired stability structure (Liu et al., 2012; Maiti et al., 2008; Malek, 2014). The parameters of the controller must be determined according to the following three design constraints (Malek, 2014)

$$Arg[G_T(j\omega_c)] = Arg[G_C(j\omega_c)G_{PDC}(j\omega_c)] = -\pi + \varphi_m \quad (26)$$

$$|G_T(j\omega_c)|_{dB} = |G_C(j\omega_c)G_{PDC}(j\omega_c)|_{dB} = 0 \quad (27)$$

$$d[Arg[G_C(j\omega)G_{PDC}(j\omega)]]/d\omega = 0 \text{ at } \omega = \omega_c \quad (28)$$

where  $\omega_c$  is the gain crossover frequency,  $\varphi_m$  is phase margin.

### Design Process of PI/PID and FOPI/FOPID Controllers

The open-loop transfer function of voltage control loop of VSI system can be written as;

$$G_{Tn}(s) = G_{Cn}(s)G_{PDC}(s) \quad (29)$$

We can get the frequency response of PI/PID and FOPI/FOPID controllers transfer function as follows;

$$G_{C1}(j\omega) = K_p + K_i/j\omega \quad (30)$$

$$G_{C2}(s) = K_p + K_i/j\omega + K_d j\omega \quad (31)$$

$$G_{C3}(s) = K_p + K_i/(j\omega)^\lambda \quad (32)$$

$$G_{C4}(s) = K_p + K_i/(j\omega)^\lambda + K_d(j\omega)^\mu \quad (33)$$

The phase and gain of controllers can be written as;

$$Arg[G_{Cn}(j\omega)] = \tan^{-1}(A_n/B_n) \quad (34)$$

where for PI controller

$$Arg[G_{C1}(j\omega)] = \tan^{-1}(A_1/B_1) = \tan^{-1}(-K_i/\omega K_p) \quad (35)$$

for PID controller

$$Arg[G_{C2}(j\omega)] = \tan^{-1}(A_2/B_2) = \tan^{-1}(K_d \omega^2 - K_i/\omega K_p) \quad (36)$$

for FOPI controller

$$Arg[G_{C3}(j\omega)] = \tan^{-1}(A_3/B_3) = \tan^{-1}\left(-K_i \omega^{-\lambda} \sin\left(\frac{\lambda\pi}{2}\right)/K_p + K_i \omega^{-\lambda} \cos\left(\frac{\lambda\pi}{2}\right)\right) \quad (37)$$

for FOPID controller



$$Arg[G_{C4}(j\omega)] = \tan^{-1}(A_4/B_4) = \tan^{-1}\left(\frac{K_d\omega^\mu \sin(\frac{\mu\pi}{2}) - K_i\omega^{-\lambda} \sin(\frac{\lambda\pi}{2})}{K_p + K_i\omega^{-\lambda} \cos(\frac{\lambda\pi}{2}) + K_d\omega^\mu \cos(\frac{\mu\pi}{2})}\right) \quad (38)$$

Also, the gain of controller is founded by (39)

$$|G_{Cn}(j\omega)| = \sqrt{(A_n)^2 + (B_n)^2} \quad (39)$$

We can express the frequency response of the transfer function of the three-phase VSI system as;

$$G_{PDC}(j\omega) = Ke^{-j\omega L}/Tj\omega + 1 \quad (40)$$

The open-loop frequency response of the controlled system is;

$$G_{Tn}(j\omega) = G_{Cn}(j\omega)G_{PDC}(j\omega) \quad (41)$$

Based on the first design specification (26), the phase of the controlled system is expressed as;

$$Arg[G_{Tn}(j\omega)] = \tan^{-1}(A_n/B_n) - \tan^{-1}(T\omega) - L\omega = -\pi + \varphi_m \quad (42)$$

Based on the second design specification (27), we can get;

$$|G_{Tn}(j\omega)| = K(\sqrt{(A_n)^2 + (B_n)^2}/\sqrt{1^2 + (T\omega)^2}) = 1 \quad (43)$$

According to third design criteria about the robustness to variation in the gain of the controlled system;

$$d(Arg(G_{Tn}(j\omega)))d\omega = [\tan^{-1}(A_n/B_n) - \tan^{-1}(T\omega) - L\omega]' = 0 \text{ at } \omega = \omega_c \quad (44)$$

### Design Process of Voltage Controller

In the simulation of the VSI system at this research, the values of resistance and inductance of output filter are, respectively,  $0.1 \Omega$ ,  $10mH$ , and DC bus voltage are  $380V$ . And also we set the sampling time at  $500kHz$ . Considering the low cut-off frequency and high sampling time, the phase delay in the system is low enough to be ignored (Malek, 2014). According to these values, the linear transfer function of the VSI system to be controlled the output voltage by an integer and fractional order controllers is;

$$G_{PDC}(s) = 1/(0.01s + 0.1) = 10(0.1s + 1) \quad (45)$$

If we want to design controllers for the voltage control loop with the frequency response method, we need to know which frequency and phase margin we will design our system. In the time response analysis of the system, we should select our damping ratio as  $\zeta = 0.707$  for 5% overshoot value. For  $0.707$  damping ratio, Liu et al. (2012) work have denoted that the optimal range crossover frequency to control the VSI system will be in the range of  $[100,640] \text{ rad/sec}$  and phase margin needs to be  $\varphi_m = 60^\circ$ .

In this research, the authors propose the cut-off frequency and phase margin of the controlled system as  $\omega_c = 200 \text{ rad/s}$ ,  $\varphi_m = 60^\circ$ . The tuned voltage controllers for  $\omega_c = 200 \text{ rad/s}$ ,  $\varphi_m = 60^\circ$  are;

$$PI(s) = 1.7 + 210s \quad (46)$$

$$PID(s) = 1.68 + 270s + 0.001s \quad (47)$$

$$FOPI(s) = 1.25 + 60s^{0.75} \quad (48)$$

$$FOPID(s) = 1.2 + 80s^{0.78} + 0.005s^{0.6} \quad (49)$$

#### 4.0 FINDINGS

In this section, the simulation result of a three-phase VSI system which is controlled by PI/PID and FOPI/FOPID voltage controller has been demonstrated. In this simulation, the power demand of dynamic load is modelled by taking energy consumed at the home between 00:00-12:00 according to Fig. 5 using hourly switching on or off the household appliance (Gül and Tan, 2019). Each hour of the day is conducted for 0.1 s at Matlab/Simulink simulations for this research.

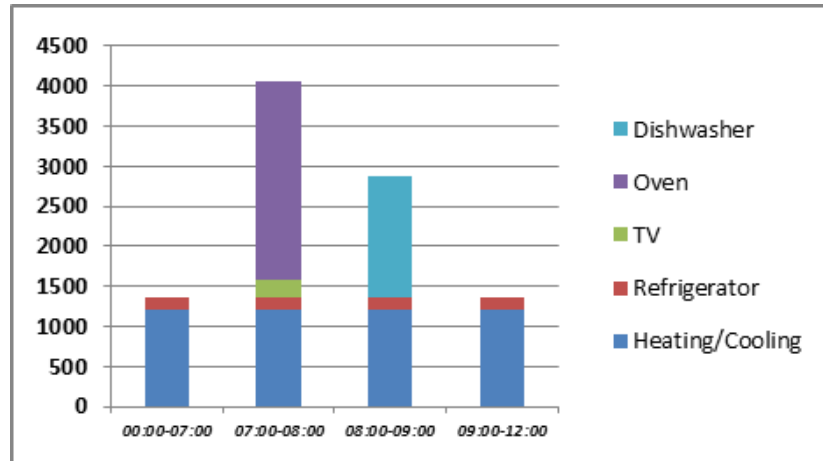


Figure 5: The Control Schematic of Voltage for the Three-Phase Inverter System Energy Consumption of Household Appliances in Watt Between 0-12 Hours

Voltage waveforms in d and q axis of VSI controlled system using PI, PID, FOPI, and FOPI are plotted for stable and unstable dynamic load conditions, respectively in Figure 6 and Figure 7. In the first scenario, it is assumed that each phase of the inverter output provides power to equal loads. Therefore, experiments ( $R_a=R_b=R_c$ ) are performed for a balanced dynamic load case. The second test scenario assumes that the VSI system drives the power load at different values for each phase ( $R_a=4/3R_b=2R_c$ ). This test scenario means an unbalanced load condition.

We set the desired amplitude of voltage reference  $V_{dref}$  to 220V and  $V_{qref}$  to 0V to make injected reactive power to be zero in this paper. By interpreting the Figure 6 and 7, we can examine the change in voltage waves ( $V_d$  and  $V_q$ ) caused by the time-varying dynamic load and perform performance analyses of the control structures used to control our system by comparing voltage waves with reference voltages ( $V_{dref}$  and  $V_{qref}$ ). Analysing these results shows the control quality of the control structures we use.

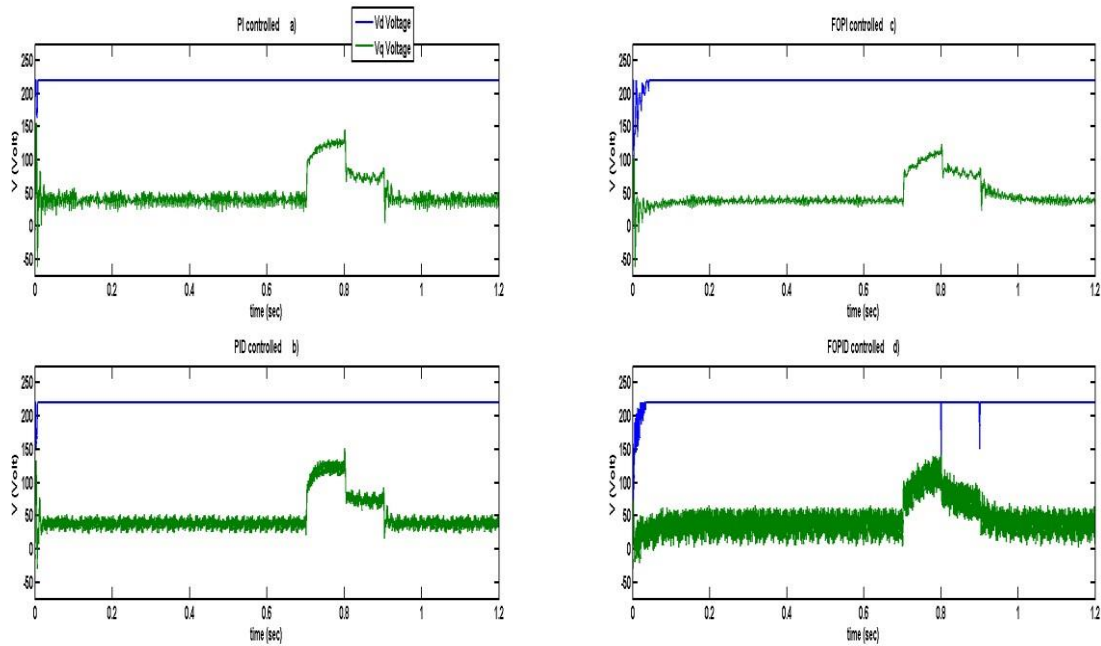


Figure 6: Inverter Output Q-Axis and D-Axis Voltages for Stable Dynamic Load Condition ( $R_a=R_b=R_c$ ) a) PI controlled system b) PID controlled system c) FOPI controlled system d) FOPID controlled system

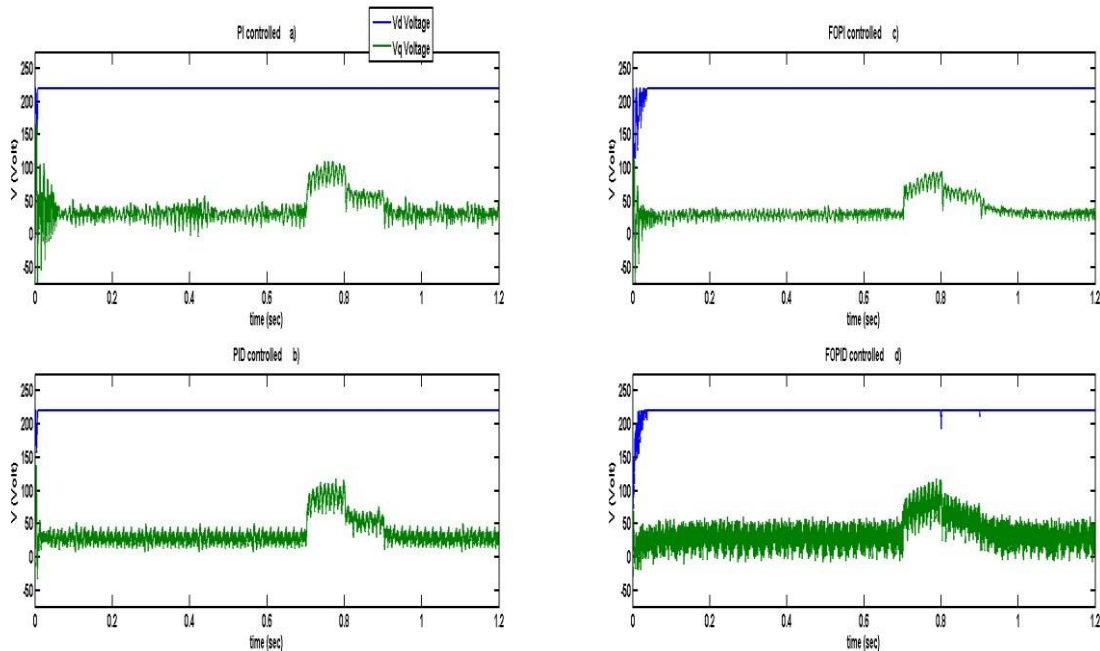


Figure 7: Inverter Output Q-Axis and D-Axis Voltages for Unstable Dynamic Load Condition ( $R_a=4/3R_b=2R_c$ ). a) PI controlled system b) PID controlled system c) FOPI controlled system d) FOPID controlled system

In Fig. 6 and Figure 7, when  $V_d$  voltage is examined, it is seen that  $V_d$  value is equal to  $V_{dref} = 220$  volt value in systems controlled by PI, FOPI, and PID control. PI, FOPI, and PID controls have been successful in controlling the  $V_d$  voltage both in the effects caused by the dynamic structure of the load and in cases where the loads at different values connected to the phase a, b and c. On the other hand, the  $V_d$  value is measured respectively, as 130 and 150 volts in the VSI system which is controlled by FOPID controller at 08:00 hour when the power consumption of household appliances decreases from 4070 watts to 2870 watts and at 09:00 hours and when become 1270 watts drops from 2870 watts for stable dynamic load condition. Also for unstable dynamic load conditions,  $V_d$  value is measured 190 volts at 08:00 hour.

When the voltage  $V_q$  in Figure 6 and 7 is investigated, it is observed that we cannot keep the  $V_q$  value at reference value 0 in all four control structures. In particular, increases in  $V_q$  are observed between 07-09 hours when load power demand rises. For stable load conditions, the highest measured  $V_q$  value was 145 volts in the PI controlled system, while the highest measured  $V_q$  value was 152, 125, and 130 volts in the PID, FOPI and FOPID controlled systems at 08:00 hour. When we examine the 6 figures more closely, it is observed that the  $V_q$  value fluctuates on average 10 volts in the PI controlled system, while  $V_q$  values vary in the range of 20 volts, 5 volts, and 50 volts respectively in PID, FOPI and FOPID controlled systems. For stable load conditions, the highest  $V_q$  values measured in PI, PID, FOPI, and FOPID controlled systems are 105 volts, 125 volts, 80 volts, 115 volts, and  $V_q$  value was observed to vary in the range of 15 volts, 30 volts, 10 volts, 50 volts.

The voltage output at the d-axis and q-axis of the inverter follows steadily a specified reference signal against uncertainties and component variations show the success of the control structure used to control the voltage control loop. In the PI/PID and FOPI/FOPID control strategies we used in our research, both stable and unstable load cases  $V_q$  components follow their references satisfactorily. However, our control strategies have not been successful in controlling the  $V_q$  component. In both stable and unstable load, unacceptable the steady-state error values occurred. Also, high oscillation at the  $V_q$  component was observed especially in PID and FOID controlled systems. Fractional-order PI controller shows better performance to control the  $V_q$  component according to less steady-state error and less oscillation when compare with PI, PID and FOPID controllers.

## 5.0 CONCLUSION AND RECOMMENDATIONS

### Conclusion

In this study, we conducted simulations to evaluate the performance of three-phase Voltage Source Inverter (VSI) systems under dynamic load conditions, employing traditional Proportional-Integral (PI), Proportional-Integral-Derivative (PID), and fractional-order Proportional-Integral-Derivative (FOPI/FOPID) voltage controllers. The dynamic load was modelled based on energy consumption patterns in a household, considering hourly switching of household appliances. Two distinct scenarios, namely a balanced load condition and an unbalanced load condition, were examined to assess the robustness of the control structures.

The voltage waveforms in the d and q axes of the VSI-controlled system were analysed for both stable and unstable dynamic load conditions. Our analysis focused on comparing the performance of PI, PID, FOPI, and FOPID controllers by examining the deviation of voltage waves from the reference voltages ( $V_{dref}$  and  $V_{qref}$ ). The desired amplitude of the voltage reference was set to 220V, with  $V_{qref}$  set to 0V to eliminate injected reactive power. The simulation results demonstrated the effectiveness of PI,



FOPI, and PID controls in maintaining the  $V_d$  voltage close to the reference value under varying load conditions. However, the FOPID controller exhibited superior performance in stabilizing  $V_d$  voltage during periods of reduced household power consumption.

In contrast, when analysing the  $V_q$  component, it was observed that none of the control structures could maintain  $V_q$  at the reference value of 0V in all scenarios. The PI control showed the most stable behaviour with an average fluctuation of 10 volts, while PID, FOPI, and FOPID controls exhibited variations in the range of 20 volts, 5 volts, and 50 volts, respectively.

### **Recommendations**

The simulation results highlighted certain challenges in controlling the  $V_q$  component, indicating steady-state errors and high oscillations, particularly in PID and FOPID controlled systems. Based on these findings, we recommend the following:

**Further Investigation into  $V_q$  Control Strategies:** Future research should focus on developing improved control strategies specifically tailored for regulating the  $V_q$  component. This may involve exploring advanced control algorithms or refining existing fractional-order control approaches.

**Adaptive Control Strategies:** Considering the dynamic nature of load conditions, adaptive control strategies should be explored to enhance the adaptability of the control system. This could involve real-time adjustments to the control parameters based on the varying load profile.

**Experimental Validation:** The simulation results provide valuable insights, but experimental validation is crucial for verifying the effectiveness of the proposed control strategies in real-world scenarios. Conducting experiments on physical VSI systems would contribute to the practical applicability of the findings.

**Integration of Machine Learning:** Incorporating machine learning techniques to the control system could enhance adaptability and self-optimization, especially in scenarios with unpredictable load variations. This could further improve the overall stability and performance of the VSI system.

In conclusion, our study delved into the performance evaluation of three-phase Voltage Source Inverter (VSI) systems under dynamic load conditions, employing various voltage controllers, including traditional Proportional-Integral (PI), Proportional-Integral-Derivative (PID), and fractional-order Proportional-Integral-Derivative (FOPI/FOPID) controllers. Through simulations representing balanced and unbalanced load scenarios, we scrutinized the behavior of the VSI controlled system, particularly focusing on the d and q axes voltage waveforms.

The findings underscored the effectiveness of PI, FOPI, and PID controls in maintaining  $V_d$  voltage close to the reference value, with the FOPID controller demonstrating superior stability during reduced household power consumption. However, challenges were identified in controlling the  $V_q$  component, revealing steady-state errors and high oscillations, particularly in PID and FOPID controlled systems.

## REFERENCES

- Åström, K. J., & Hägglund, T. (2009). *Advanced PID Control*. Pearson-Prentice Hall.
- Gül, O., & Tan, N. (2019). Application of Fractional Order Voltage Controller in Building Integrated Photovoltaic and Wind Turbine. *Measurement and Control*, 52(7-8), 1145-1154.
- Guzmán, J. L., Åström, K. J., Dormido, S., Hägglund, T., & Piguet, Y. (2006). Interactive learning modules for PID control. *IFAC Proceedings Volumes*, 39(6), 7-12.  
<https://doi.org/10.3182/20060621-3-US-00003>
- Karabiber, A., Keleş, C., Kaygusuz, A., Alagöz, B. B., & Akçın, M. (2016). Power Converters Modeling in Matlab/Simulink for Microgrid Simulations. 4th International Istanbul Smart Grid and Cities Congress and Fair Energy and Building, 1-5.  
<https://doi.org/10.1109/SGCF.2016.7492418>
- Liu, S., Bi, T., Xue, A., & Yang, Q. (2012). An Optimal Method for Designing the Controllers Used in Grid-Connected PV Systems. *Proceedings of the IEEE International Conference on Power System Technology (POWERCON)*. <https://doi.org/10.1109/PowerCon.2012.6401339>
- Maiti, D., Acharya, A., Chakraborty, M., Konar, A., & Janarthanan, R. (2008). Tuning PID and Fractional PID Controllers using the Integral Time Absolute Error Criterion. 4th International Conference on Information and Automation for Sustainability, 457-462.  
<https://doi.org/10.1109/ICIAFS.2008.4783932>
- Malek, H. (2014) *Control of Grid-Connected Photovoltaic Systems Using Fractional Order Operators*. (Doctoral dissertation). Utah University, Utah.
- Mohan, N. (1995). *Power Electronics-Converters Application and Design*. John Wiley & Sons Inc.
- Mu, K., Ma, X., Mu, X., & Zhu, D., (2011). Study on Passivity-Based Control of Voltage Source PWM DC/AC Inverter. International Conference on Electronic & Mechanical Engineering and Information Technology, Harbin, China. 3963-3967.  
<https://doi.org/10.1109/EMEIT.2011.6023889>
- Yang, B., Yu, T., Shu, H., Dena Zhu, D., Na, A., Sang, Y., & Jiang, L. (2018). Energy reshaping based passive fractional-order PID control design and implementation of a gridconnected PV inverter for MPPT using grouped grey wolf optimizer. *Solar Energy*, 170, 31-46.  
<https://doi.org/10.1016/j.solener.2018.05.034>

## License

Copyright (c) 2024 Ozan Gül



This work is licensed under a [Creative Commons Attribution 4.0 International License](https://creativecommons.org/licenses/by/4.0/). Authors retain copyright and grant the journal right of first publication with the work simultaneously licensed under a [Creative Commons Attribution \(CC-BY\) 4.0 License](https://creativecommons.org/licenses/by/4.0/) that allows others to share the work with an acknowledgment of the work's authorship and initial publication in this journal.